Global Markov modelling and analysis of granular flow dynamics

Gary Froyland*, Antoinette Tordesillas† and David M. Walker†

*School of Mathematics and Statistics, University of New South Wales, Sydney NSW 2052, Australia
†Department of Mathematics and Statistics, University of Melbourne, Parkville VIC 3010, Australia

Abstract. Granular flows are highly complex interconnected dynamical systems that are deterministic, but difficult to predict at a microscopic level over even modest periods of time. One of the most useful mathematical approaches to analyse such microscopically chaotic systems is based upon considering the flow of densities (or ensembles of particles) rather than individual particles. In recent years, these techniques have been honed to offer an efficient means of identifying stable macroscopic structures despite the unpredictability at the microscopic level. The numerical methodology is based around the concept of a transition matrix that describes the dynamics on a user-selected state space. For example, in granular flows, the state space may be a continuous space of particle stabilities, or a discrete space describing particle-neighbour interactions, or any one of many other possibilities; the transition matrix describes transitions between different particle states. These methods have previously been applied in a variety of other application settings, including molecular dynamics and physical oceanography.

Keywords: Granular materials, dynamical system, transition matrix, ensemble dynamics, Markov model
PACS: 81.05Rm

INTRODUCTION

We begin by considering dynamical systems in a flexible abstract framework that is adaptable to myriad settings in granular flow. For our purposes, a dynamical system (X,T) consists of a *domain* X, and a *map* $T : X \to X$ that describes the dynamics on the domain by mapping a particular point $x \in X$ to $T(x) \in X$, representing the passage of one unit of time. In the granular flow context, the set X might be (i) a discrete set of individual granular particle *motifs* representing local neighbour topologies, or (ii) an interval of possible stability values of individual granular particles computed from local neighbours, and T is the effect of some external input/forces on the states $x \in X$ of individual granular particles. Figure 1 shows the motifs of a central particle before and after k steps of the dynamics.

The domain X will be endowed with a *metric* $D : X \times X \to \mathbb{R}^+$, which quantifies the "distance" between two points in X. In the motif example, D is a discrete metric on the motifs; $D(x,x) = 0$ and $D(x,y) = 1$ if $x \neq y$, while in the other examples, D is the usual Euclidean metric. The *diameter* of X can be defined as $D^* := \max_{x,y \in X} D(x,y)$.

Complex dynamical systems often display behaviour that is complicated and difficult to predict over short time-frames. By the system (X,T) being "difficult to predict" we mean that if $D(x,y)$ is initially small relative to D^* then $D(T^k x, T^k y)$ typically grows rapidly for $k = 1,\ldots,K$ at which point $D(T^K x, T^K y)$ becomes of the order of D^* (note that K depends on x and y). Thus,

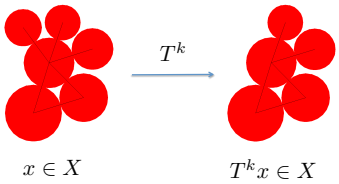

FIGURE 1. A central particle and its contacting neighbours define an individual motif $x \in X$. Throughout deformation in response to the load, particles rearrange to form a new configuration after k loading steps $T^k x$. We are interested in quantifying the number of different motifs (size of set X), the frequency with which different motifs occur, and the frequency of motif-to-motif transitions.

if there is a small error in an initial state x, due to experimental observation or other source, so that the recorded state is x', under iteration of the dynamics, the distance between $T^k(x)$ and $T^k(x')$ grows rapidly until it reaches D^*; after this time future predictions are meaningless; these notions go back to Lorenz [1] and contemporaneous works. One frequently observes that the rapid growth from $k = 1,\ldots,K$ can be best modelled as geometric growth, so that $D(T^k x, T^k y) \approx C\rho^k D(x,y)$, $k = 1,\ldots,K(x,y)$ for a modest constant C and $\rho > 1$. It is this geometric growth property that makes prediction of individual particle trajectories difficult beyond the short term.

In terms of granular flow dynamics, one wishes to choose X in such a way that a single point $x \in X$ is a good

descriptor of the current state of the granular particles. The choice of metric D is up to the modeller and should reflect the fact that two points in X are close according to D if the corresponding properties of the two granular particles are similar.

ENSEMBLES AND COARSE-GRAINING

Despite the unpredictability of individual *trajectories* $x, T(x), T^2(x), \ldots$, if one considers an *ensemble* of initial points in X, then the evolution of this ensemble under the dynamics is typically *highly predictable*, converging to a *stationary ensemble* that is invariant under the dynamics.

For simplicity, and sympathy with our numerical calculations, we will consider discrete ensembles formed by coarse-graining X. This coarse-graining is constructed by partitioning X into regions (called *boxes*) $B_1, \ldots, B_n$ so that $B_i \cap B_j = \emptyset$, $i \neq j$, and $\bigcup_{i=1}^n B_i = X$. We will also like each B_i to be representative of a particular "region" of the domain X and so ideally, the diameter of each B_i should be small, according to the metric D.

We now begin to build a probabilistic model of T (in fact, a Markov chain) on the coarse-grained partition $\{B_1, \ldots, B_n\}$. This probabilistic model will be governed by an $n \times n$ transition matrix P, where the number P_{ij} is the (conditional) probability of a point $x \in B_i$ moving to B_j under the action of T, given the information that $x \in B_i$. Since the boxes partition X, and $T(x)$ has to lie in one of the boxes, one has $\sum_{i=1}^n P_{ij} = 1$ for each $i = 1, \ldots, n$.

If X is a discrete, finite set $\{x_1, \ldots, x_r\}$ then we define

$$P_{ij} = \frac{\#\{k : x_k \in B_i, T(x_k) \in B_j\}}{\#\{x_k \in B_i\}}, \qquad (1)$$

where $\#A$ denotes the cardinality of the set A. In the context of granular flows where X is an interval of particle stabilities, we use exactly the above construction.

If X is a continuum, we need to impose a little more structure; the easiest case is where $X \subset \mathbb{R}^d$ and X inherits the standard notion of volume in Euclidean space. In this case, we define

$$P_{ij} = \frac{vol(B_i \cap T^{-1}B_j)}{vol(B_i)}. \qquad (2)$$

Notice that in both (1) and (2), the numerator represents the size of the set of points that are currently in B_i and will be in B_j after one application of the dynamics T.

For the situation where X is a collection of particle motifs, we have to slightly modify the above constructions because there can be several particles that share the same motif. Formally, there is a motif function $\pi : \{1, \ldots, r\} \to X$ that maps each one of the granular particles to its motif, and this function π is not one-to-one. Thus, we must count the motif transitions with particle multiplicity and define

$$P_{ij} = \frac{\#\{1 \leq k \leq r : \pi(k) \in B_i, \pi(k') \in B_j\}}{\#\{1 \leq k \leq r : \pi(k) \in B_i\}}, \qquad (3)$$

where $\pi(k')$ refers to the property of particle k after one time-step. Because π isn't one-to-one there is no formal description of a map T on X, but from the point of view of probabilistic modelling, this is not a problem.

The coarse-grained matrix constructions above have a long history, going back to Ulam [2]. Hsu [3] introduced the related cell-to-cell mapping for dynamical systems, Dellnitz *et al.* [4] introduced an efficient computational framework; see [5] for a survey of these methods.

Ensemble dynamics

An ensemble on our coarse-grained space $\{B_1, \ldots, B_n\}$ is represented by an $n \times 1$ probability vector p, where $p \geq 0$, and $\sum_{i=1}^n p_i = 1$. The number p_i represents the probability that a randomly chosen point in X is contained in B_i.

Given some initial ensemble p^0, we can apply the map T at the level of ensembles by matrix multiplication by P; that is $p^1 = p^0 P$. The new ensemble p^1 is the result one obtains by taking the ensemble p^0 and applying T to every point in that ensemble. If we wish to calculate p^ℓ for some large ℓ, we construct the matrix P from a *single* iteration of T, and then by vector/matrix multiplication iteratively apply the rule $p^{k+1} = p^k P$, $k = 0, \ldots, \ell - 1$. The mechanics of this operation is incredibly simple and fast once the transition P has been constructed. It is much more efficient than individually applying T^ℓ to all points $x \in X$ and then finally coarse-graining.

THE INVARIANT ENSEMBLE

Under rather mild conditions, namely that there is some $k > 0$ for which $P^k > 0$ (dynamically, this roughly means that the k-fold images of each box B_i are eventually intersecting all other boxes B_j), the Perron-Frobenius theorem [6] guarantees that the coarse-grained dynamics has a unique, stable, invariant ensemble p^∞. The ensemble p^∞ has the property that any initial ensemble p^0 eventually converges to it: $p^0 P^k \to p^\infty$, and the property that it is invariant under the coarse-grained dynamics: $p^\infty P = p^\infty$ (p^∞ is the unique eigenvector with eigenvalue 1).

The invariant probability vector or *invariant ensemble* p^∞ is trivial to compute as the eigenvector of eigenvalue 1 of P. This ensemble describes the time-asymptotics of the dynamical system, not only in the sense of ensemble dynamics (all initial ensembles, when evolved forward in time, converge to p^∞), but also has an interpretation in terms of the dynamics of (X, T). Select an $x \in X$ and

compute an infinite trajectory $x, T(x), T^2(x), \ldots$. Now for any box B_i, calculate the relative frequency with which the trajectory enters B_i:

$$freq_i := \lim_{\ell \to \infty} \frac{\#\{k : T^k(x) \in B_i, 0 \le k \le \ell - 1\}}{\ell}.$$

Then $freq_i \approx p_i$ and under certain conditions it can be proved that $freq_i \to p_i$ as the diameters of the boxes B_i go to zero (the coarse-graining is refined); see the survey [5] for details and further references. Thus, the invariant ensemble p^∞ provides valuable time-asymptotic information that would otherwise be expensive to estimate by explicitly computing long trajectories. In the context of granular flow, the invariant ensemble provides important information on the relative frequencies at which eg. different motifs and stability values occur.

ALMOST-INVARIANT SETS

In this section we describe how to decompose X into regions that are close to invariant under short periods of time. We say that a set $A \subset X$ is *invariant* if $A = T^{-1}A$. In the context of particle motifs, an invariant set would be a subcollection of motifs that cycle amongst themselves under the shear action, never turning into a motif outside the subcollection, while in the context of particle stability values, an invariant set would be a subinterval of stability values which remains unchanged under the shear action.

We will use our boxes $\{B_1, \ldots, B_n\}$ to construct these regions; if the diameters of our boxes are small, we can well-approximate any subset of X by unions of boxes. Let $A = \bigcup_{i \in I_A} B_i$, where $I_A \subset \{1, \ldots, n\}$ is the set of indices of boxes that make up the set A. We will call the set A *almost-invariant* (the definition below is a refinement of the original notion [7]; see [8]) if

$$\rho(A) := \frac{\sum_{i \in I_A} \sum_{j \in I_A} p_i^\infty P_{ij}}{\sum_{i \in I_A} p_i^\infty} \tag{4}$$

is close to 1. The numerator in (4) represents the conditional probability (according to ρ^∞) of a trajectory of T being in A at the present time, and one step in the future, given that the trajectory is currently in A. Obviously the closer $\rho(A)$ is to 1, the larger the almost-invariance and the closer A is to being invariant.

It is natural to ask how best one can partition X into two sets A and $A^c = X \setminus A$ so that both A and A^c have the largest possible values for $\rho(A)$ and $\rho(A^c)$. That is, what is $\max_{A \subset X} \min\{\rho(A), \rho(A^c)\}$, where A is formed from a union of boxes? An excellent heuristic to solve this optimisation problem uses the spectral information of the transition matrix P. These techniques have been used in the ocean dynamics [9] and molecular dynamics [10] settings to accurately map oceanic gyres and find molecular conformations, respectively, as almost-invariant sets.

To take advantage of optimality properties of eigenvectors of symmetric matrices, it is beneficial to introduce the matrix $\hat{P}$, defined by $\hat{P}_{ij} = \frac{p_j^\infty P_{ji}}{p_i^\infty}$. The matrix $\hat{P}$ is well-known in classical Markov chain theory (see eg. [11]) as the reverse-time chain governed by P. The matrices P and $\hat{P}$ share the same invariant probability vector p^∞ and crucially, it is easy to check that if one computes $\rho(A)$ with $\hat{P}$ in place of P, the value of $\rho(A)$ is unchanged. Thus almost-invariance with respect to the invariant ensemble p^∞ is independent of the direction of flow of time.

We now define a matrix $R = (\hat{P} + P)/2$, which is row-stochastic, has p^∞ as its invariant probability vector, satisfies $R = \hat{R}$, and computing $\rho(A)$ with R in place of P yields no change. The matrix R is now symmetric with respect to a weighted (by p^∞) inner product, has real spectrum, and its eigenvectors enjoy certain optimisation properties (Rayleigh-Ritz Minimax Theorem [11]). If $\lambda_{2,R}$ denotes the second largest eigenvalue of R, then

$$1 - \sqrt{1 - \lambda_{2,R}} \le \max_{A \subset X} \min\{\rho(A), \rho(A^c)\} \le (1 + \lambda_{2,R})/2. \tag{5}$$

These bounds and the above constructions may be found in [8] (justification for the "min" expression may be found in [12]), and are based on conductance bounds for reversible Markov chains [13, 11].

The second right eigenvector v_2 of R is used to partition X. In the simplest version of the heuristic, one partitions X as $A = \bigcup_{i : v_{2,i} \ge 0} B_i$ and $A^c = \bigcup_{i : v_{2,i} < 0} B_i$. One can improve on this by optimising the threshold to maximise the ρ values; that is, consider $A_b = \bigcup_{i : v_{2,i} \ge b} B_i$ and $A_b^c = \bigcup_{i : v_{2,i} < b} B_i$, and select b so that $\min\{\rho(A_b), \rho(A_b^c)\}$ is maximal.

Extending the above principle, one can use information from eigenvectors $v_2, v_3, \ldots, v_k$ of R to subdivide X into k almost-invariant sets. One now has $k-1$ "thresholds" to find. Considering the entries $V_k := \{(v_{2,i}, \ldots, v_{k,i}) : i = 1, \ldots, n\}$ as a set of points in $\mathbb{R}^{k-1}$, we group these points by a clustering algorithm to find a partition. As in [8], we use a weighted fuzzy clustering algorithm, weighted by the invariant ensemble weights so that each cluster has small radius in $\mathbb{R}^{k-1}$ and approximately similar weight.

We illustrate these ideas via a 2D constant volume cyclic shear test of >1000 bidisperse photoelastic disks (see [14] and references therein). In the context of particle motifs, Figure 2(a) shows V_k for $k = 3$ as a subset (consisting of 28 points corresponding to the 28 motifs) of $\mathbb{R}^2$ with each cluster indicated by a different colour. Figure 2(b) shows the results of the clustering algorithm to partition the motif collection into ℓ sets by finding ℓ clusters in V_k, $1 \le k \le \ell$.

The determination of these almost-invariant sets of

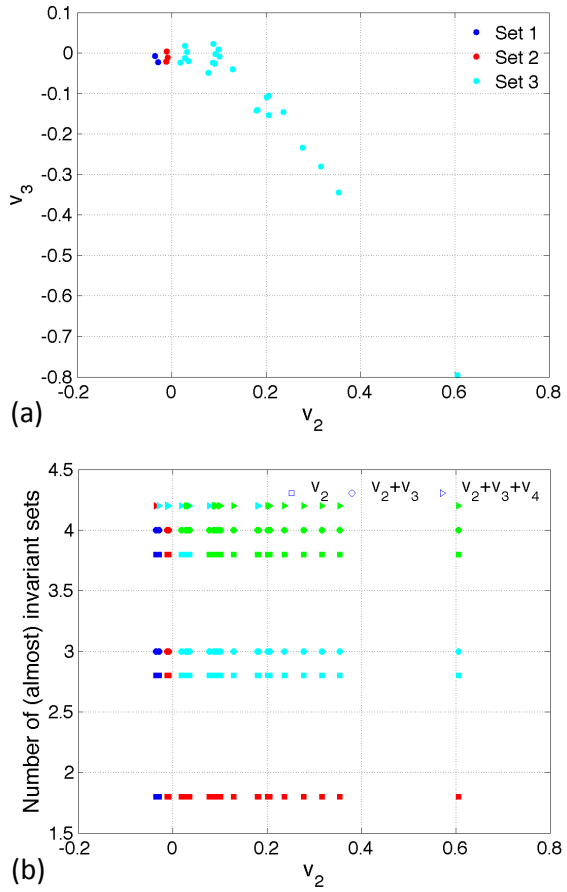

FIGURE 2. (a) The result of clustering the motifs into three disjoint sets using the information in eigenvectors v_2 and v_3. (b) Almost-invariant set membership determination from eigenvector information. The information in v_2 is sufficient to determine two almost-invariant sets. These sets can further partitioned into three or four disjoint subsets (square) using only v_2, however, exploiting additional eigenvectors can improve the clustering (circle and triangle).

motifs is crucial for the formulation of robust predictive continuum modelling. If we can identify the most likely configurations a granular material can access *and* determine the most likely configurational changes such groups of particles take part in, then we can more accurately scale up models to the macroscopic level. For example, in [15], modelling only one configurational change based on the confined buckling of force chains successfully captured macroscopic trends. The techniques presented herein and in [14] enable identification of additional configurational changes and mechanisms to consider when modelling from the particle-scale to the macroscopic-scale.

In summary, the approach of constructing a Markov chain model via coarse-graining is an extremely flexible modelling approach, enabling one to efficiently estimate invariant ensembles and almost-invariant sets. The latter directly reveal stable macroscopic structures in the model domain, which are virtually invisible to direct computational methods that use individual trajectory information. Future work will consider mobile versions of almost-invariant sets, allowing one to identify time-dependent stable macroscopic structures from models with time-varying dynamics.

ACKNOWLEDGMENTS

We thank R.P. Behringer for continued access to his experimental data. GF is partially supported by ARC DP110100068. AT & DMW are partially supported by the US Army Res. Off. (W911NF-11-1-0175), ARC DP120104759, and the Melbourne Energy Institute.

REFERENCES

1. E. N. Lorenz, *Journal of the Atmospheric Sciences* **20**, 130–141 (1963).
2. S. Ulam, *Problems in Modern Mathematics*, Interscience, 1964.
3. C. S. Hsu, *Cell-to-cell mapping: a method of global analysis for nonlinear systems*, Springer-Verlag, New York, 1987.
4. M. Dellnitz, G. Froyland, and O. Junge, "The algorithms behind GAIO – Set oriented numerical methods for dynamical systems," in *Ergodic Theory, Analysis, and Efficient Simulation of Dynamical Systems*, edited by B. Fiedler, Springer, 2001, pp. 145–174.
5. G. Froyland, "Extracting dynamical behaviour via Markov models," in *Nonlinear Dynamics and Statistics: Proceedings, Newton Institute, Cambridge, 1998*, edited by A. I. Mees, Birkhäuser, 2001, pp. 283–324.
6. A. Berman, and R. Plemmons, *Nonnegative matrices*, SIAM, 1979.
7. M. Dellnitz, and O. Junge, *Int. J. Bif. and Chaos* **7**, 2475–2485 (1997).
8. G. Froyland, *Physica D* **200**, 205–219 (2005).
9. G. Froyland, K. Padberg, M. H. England, and A. M. Treguier, *Physical Review Letters* **98**, 224503 (2007).
10. C. Schütte, W. Huisinga, and P. Deuflhard, "Transfer Operator Approach to Conformational Dynamics in Biomolecular Systems," in *Ergodic Theory, Analysis, and Efficient Simulation of Dynamical Systems*, edited by B. Fiedler, Springer, Berlin, 2001, pp. 191–223.
11. P. Brémaud, *Markov chains. Gibbs fields, Monte Carlo simulation, and queues*, Springer, New York, 1999.
12. G. Froyland, and K. Padberg, *Physica D* **238**, 1507–1523 (2009).
13. A. Sinclair, and M. Jerrum, *Information and Computation* **82**, 93–133 (1989).
14. A. Tordesillas, D. M. Walker, G. Froyland, J. Zhang, and R. P. Behringer, *Physical Review E* **86**, 011306 (2012).
15. A. Tordesillas, and M. Muthuswamy, *Journal of the Mechanics and Physics of Solids* **57**, 706–727 (2009).